NRAV, a Long Noncoding RNA, Modulates Antiviral Responses through Suppression of Interferon-Stimulated Gene Transcription

Jing Ouyang,[1] Xiaomei Zhu,[1,2] Yuhai Chen,[1] Haitao Wei,[1] Qinghuang Chen,[1,3] Xiaojuan Chi,[3] Baomin Qi,[3] Lianfeng Zhang,[4] Yi Zhao,[5] George Fu Gao,[1] Guoshun Wang,[6] and Ji-Long Chen[1,3,*]

[1]CAS Key Laboratory of Pathogenic Microbiology and Immunology, Institute of Microbiology, Chinese Academy of Sciences, Beijing 100101, China
[2]School of Life Sciences, Anhui University, Hefei 230601, China
[3]College of Animal Sciences, Fujian Agriculture and Forestry University, Fuzhou 350002, China
[4]Institute of Laboratory Animal Science, Chinese Academy of Medical Sciences & Comparative Medical Center, Beijing 100021, China
[5]Key Laboratory of Intelligent Information Processing, Institute of Computing Technology, Chinese Academy of Sciences, Beijing 100190, China
[6]Gene Therapy Program, Departments of Microbiology and Immunology, Medicine and Genetics, Louisiana State University Health Sciences Center, New Orleans, LA 70112, USA
*Correspondence: chenjl@im.ac.cn
http://dx.doi.org/10.1016/j.chom.2014.10.001

SUMMARY

Long noncoding RNAs (lncRNAs) modulate various biological processes, but their role in host antiviral responses is largely unknown. Here we identify a lncRNA as a key regulator of antiviral innate immunity. Following from the observation that a lncRNA that we call *negative regulator of antiviral response* (NRAV) was dramatically downregulated during infection with several viruses, we ectopically expressed NRAV in human cells or transgenic mice and found that it significantly promotes influenza A virus (IAV) replication and virulence. Conversely, silencing NRAV suppressed IAV replication and virus production, suggesting that reduction of NRAV is part of the host antiviral innate immune response to virus infection. NRAV negatively regulates the initial transcription of multiple critical interferon-stimulated genes (ISGs), including IFITM3 and MxA, by affecting histone modification of these genes. Our results provide evidence for a lncRNA in modulating the antiviral interferon response.

INTRODUCTION

Thousands of lncRNAs are pervasively transcribed in mammalian cells. Accumulating data indicate that they are an important class of regulatory RNAs in a variety of cellular processes (Mercer et al., 2009). To serve the function of signaling, decoying, scaffolding, or guiding, lncRNAs employ their motifs to interact with other molecules (Guttman and Rinn, 2012; Wang and Chang, 2011). Most recently, three lncRNAs (murine NeST, human THRIL, and NEAT1) are shown to regulate the innate immunity by modulating the transcription of IFN-γ, TNF-α, and

IL8, respectively (Cullen, 2013; Gomez et al., 2013; Imamura et al., 2014; Li et al., 2014). In addition, mouse lincRNA-Cox2 plays a central role in control of the Pam3CSK4-induced inflammatory response (Carpenter et al., 2013). Whole transcriptome studies have also demonstrated the differential expression of lncRNAs in SARS coronavirus-infected mice (Peng et al., 2010) and enterovirus 71-infected RD cells (Yin et al., 2013), suggesting the functional involvement of lncRNAs in antiviral immunity. Interestingly, several lncRNAs have been shown to modulate viral infection. For example, 7SL and NEAT1 are evidenced to interfere with the HIV-1 virion package and posttranscriptional expression (Wang et al., 2007; Zhang et al., 2013). lncRNA VIN can facilitate influenza A virus (IAV) propagation (Winterling et al., 2014). Despite these progresses, the specific functions of these lncRNAs in the host defense process remain incompletely characterized.

IAV infection poses a significant threat to global health (Mänz et al., 2013), but the mechanisms underlying IAV-host interaction are still elusive. Host anti-IAV response is initiated by the recognition of viral components by pathogen recognition receptors (PRRs), such as retinoic acid-inducible gene I (RIG-I), melanoma differentiation factor 5 (MDA5), and toll-like receptor 3 (TLR3). Through the signaling cascade downstream the stimulated receptors, transcription factors including IRF3/7 and NF-κB are activated. Type I and III interferons (IFNs) are then rapidly produced, which induce the synthesis of hundreds of antiviral proteins encoded by IFN-stimulated genes (ISGs). Consequently, the accumulation of ISG proteins in cytosol, including the well-known IFN-induced protein with tetratricopeptide repeats IFIT2, IFIT3 (Fensterl et al., 2012; Liu et al., 2011), IFN-induced transmembrane protein 3 (IFITM3) (Everitt et al., 2012), and myxovirus resistance 1 (human MxA or mouse Mx1) (Mänz et al., 2013), provides antiviral protection through multiple mechanisms. Importantly, modulation of anti-IAV immunity epigenetically has emerged to be a critical mechanism. After the activation of transcription factors, a transcriptional regulation cascade is triggered (Smale, 2012). The cascade includes

multiple waves of transcriptional activation and inhibition controlled by a complex network. First of all, regulations of promoter activity and chromatin structure are essential steps for the transcription initiation. For example, the activation of the promoters of immune genes *ifit2*, *ifit3*, and *mx1* requires nucleosome remodeling through SWItch/Sucrose NonFermentable (SWI/SNF) complexes and histone modifications (H3K4me3 or H3K9/K14ac) (Ramirez-Carrozzi et al., 2009). IFN-γ promoter is reported to be upregulated by lncRNA NeST, which binds with H3K4 methylase complex component WDR5 to alter histone methylation levels (Gomez et al., 2013). In addition, the mRNA maturation and stabilization are also critical posttranscriptional regulation steps. Heterogeneous nuclear ribonucleoproteins (hnRNPs) regulate gene transcription and subsequent modification of the newly synthesized RNA (pre-mRNA) in nucleus. Recent studies have shown that hnRNP L and hnRNP A/B are associated with the induction of immunity genes TNF-α and CCL5 through interaction with lncRNA THRIL and lincRNA-Cox2, respectively (Carpenter et al., 2013; Li et al., 2014). These data suggest that additional coregulators are required for transcriptional activation/inhibition of innate immunity genes.

In this study, genome-wide profiling of lncRNA expression identified a human lncRNA, designated NRAV, that played a critical role in anti-IAV infection. In vitro and in vivo data showed that NRAV functioned as a negative regulator in the host antiviral immunity by repression of ISG production through strict control of the transcription rate. Furthermore, we found that NRAV regulated the expression of MxA and IFITM3, likely through affecting histone modification of their genes. These results reveal a layer of the regulation of host innate defense during the IAV infection.

RESULTS

Human NRAV Is Identified as a lncRNA Controlling Virus Infection

To investigate the roles of host lncRNAs in IAV infection, genome-wide lncRNA microarrays were performed of human alveolar epithelial cells (A549) infected with or without influenza virus A/WSN/33 (H1N1) for 12 hr. A total of 494 upregulated and 413 downregulated lncRNAs following the viral infection were detected (fold change >2) and clustered (Figure 1A, left). Nine lncRNAs were selected as candidates after an in silico screen (see Supplemental Information available online) and confirmation by RT-PCR (Figure 1A, right).

To identify the functional lncRNAs, viral activity screening was performed (Figures S1A and S1B). lncRNA NRAV was found to affect the virus replication most significantly, and thus it was chosen for in-depth study. The human lncRNA gene *nrav* (LOC100506668, uc001tyk, also named as *dynll1-as1*) is located on chromosome 12q24.31, overlapping with the antisense strand of dynein light chain coding gene *dynll1* within intron 1 (Figure 1B). No protein-coding potential was found in NRAV by analysis using ORF Finder (NCBI), coding potential calculator (score is −0.743) (Figure S1C), and PhyloCSF (score is −3452) (Lin et al., 2011). Using polysome analysis, we further observed that NRAV displayed different distribution patterns in sucrose gradient fractions as compared with control protein-coding mRNA of GAPDH that locates in the same fractions as polysome, demonstrating the noncoding potential of NRAV (Figures S1D

and S1E). Importantly, both qRT-PCR and northern blotting confirmed that NRAV expression was markedly reduced in IAV-infected A549 cells (Figures 1C and 1D). Northern blot analysis using a specific probe (793 nt) demonstrated that the major form of human NRAV was the transcript of approximately 1,200 nt (Figure 1D). Consistently, determination of 5′ and 3′ ends of NRAV by RACE studies revealed that NRAV transcript is exactly 1,176 nt and contains a polyadenylated (12 As) tail (Figures 1E and S1F; Table S1).

Furthermore, we observed that NRAV was downregulated in a virus dose- and infection time-dependent manner (Figure 1F). Interestingly, NRAV was expressed in various human cell lines, and its expression was dramatically reduced after IAV infection in all examined cell lines susceptible to the infection, but not in cell lines (HeLa, HepG2) less permissive to IAV replication (Figure 1G). Surprisingly, NRAV was also significantly downregulated by infections of several other viruses, including a negative ssRNA virus Sendai virus (SeV), a dsRNA virus Muscovy Duck Reovirus (MDRV), and a DNA virus herpes simplex virus (HSV) (Figures 1H and 1I). In contrast, NRAV levels were not affected by pseudovirus transduction, LPS treatment, etoposide stimulation, or serum withdrawal (Figures S1G–S1J). Together, these experiments demonstrate that reduction of NRAV level is associated with viral infection.

In addition, we identified NRAV homolog-coding sequences in monkey and mouse genomes through Blast (NCBI) in silico analysis. However, we only detected NRAV homolog transcript in monkey Vero cells, but not in mouse cells by RT-PCR (Figures S1K and S1L). These results suggest that the *nrav* gene may be conserved but evolved to be differentially regulated.

Altering NRAV Expression Has Profound Effects on IAV Replication in Human Cells

To further determine the functionality of NRAV in IAV infection, we generated A549 and 293T cell lines stably expressing whole length of the human NRAV or specific shRNAs targeting NRAV using the retroviral vectors or shRNA-based lentivectors (Figures 2A, S2A, and S2B). Although IAV infection reduced the endogenous NRAV expression, it had no significant effects on the ectopically expressed NRAV and could not diminish the difference of NRAV expression between sh-Luc control cells and NRAV knockdown cells (Figure 2B). Strikingly, both the virus growth kinetics measured by haemagglutination assay and the virus titers determined by plaque-forming test showed that forced expression of NRAV significantly promoted the viral replication, while disruption of NRAV expression consistently impaired the virus reproduction in A549 cells (Figures 2C–2E). The sh-NRAV-1 cells with lower NRAV expression were used in further studies. Similar results were obtained from NRAV overexpression and knockdown in 293T cells (Figure S2C). The increased virus titers in supernatant from NRAV-overexpressing cells were further confirmed by western blotting using an antibody against the IAV hemagglutinin (HA) (Figures S2D and S2E). Because IAV infection caused a marked decrease in NRAV expression in A549 cells, we determined whether NRAV levels in NRAV-knockdown cells were lower than those in the control cells during IAV infection. Indeed, the knockdown cells showed clearly low levels of NRAV compared with the controls (Figure 2F). However, the DYNLL1 levels were not affected by
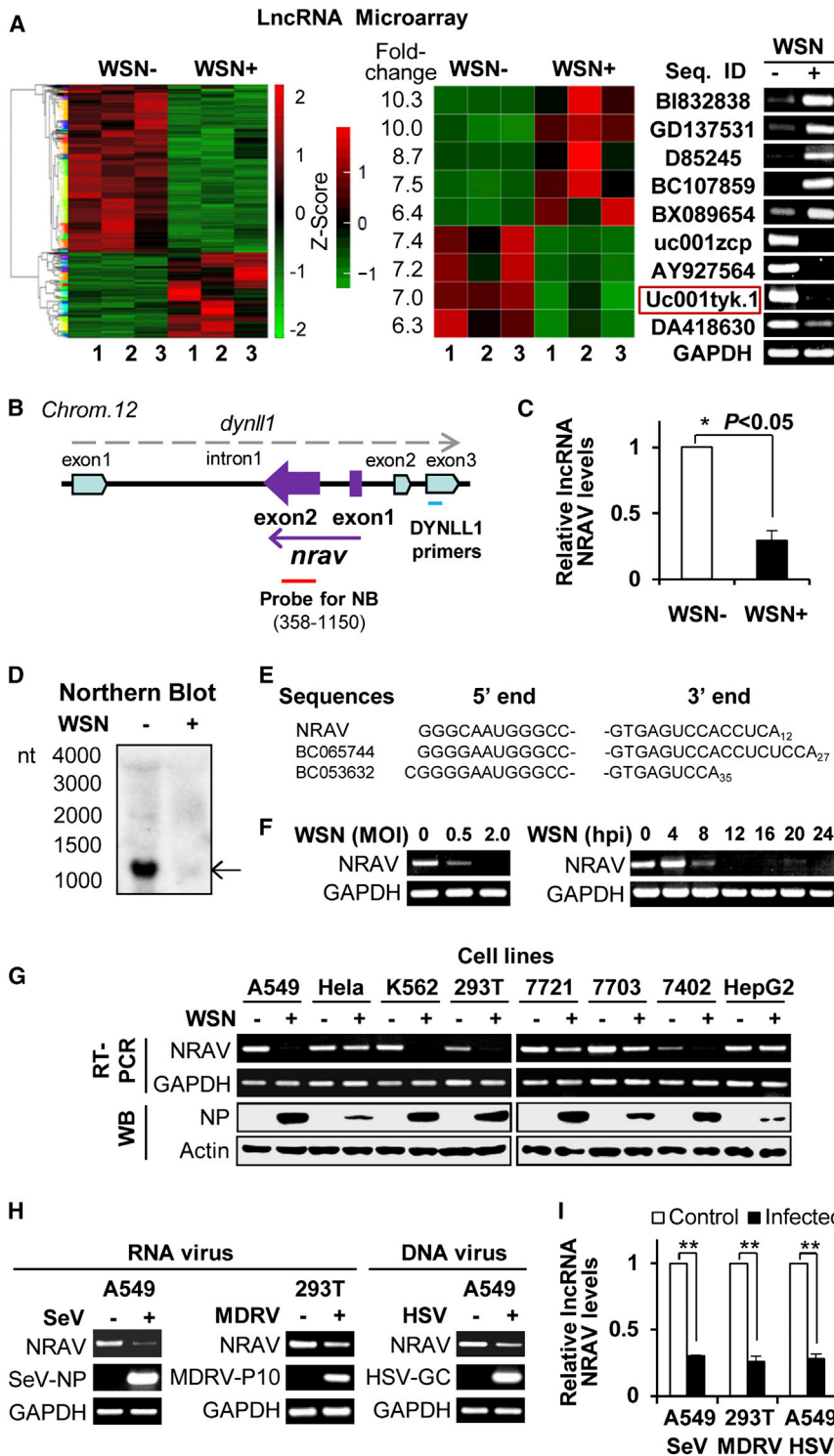
A LncRNA Microarray

Figure 1. Human NRAV Is Identified as a lncRNA Involved in Virus Infection

(A) Microarray analysis revealed 494 upregulated and 413 downregulated lncRNAs in IAV-infected A549 cells compared to control (n = 3; fold change > 2.0; p < 0.05) (left). Cells infected with WSN were collected 12 hr postinfection (hpi). The RNA quantitation is shown as centered and scaled log2 data in heatmaps. The differential expressions of 9 selected lncRNAs were confirmed by RT-PCR (right). NRAV (uc001tyk.1) is indicated by red rectangle.

(B) Shown is a paradigm of the genomic location of lncRNA gene *nrav* (purple) and the relationship with gene *dynll1* (light blue). The probe for NRAV used in northern blot (NB) (red bar) and the primers for DYNLL1 (blue bar) are indicated (not scaled).

(C and D) The downregulation of NRAV in infected A549 cells was confirmed by qRT-PCR (C) (n = 3; means ± SEM; *p < 0.05) and northern blot (D). Arrow indicates the abundant form of NRAV.

(E) The 5′ and 3′ end sequences of NRAV in A549 determined by 5′ and 3′ RACE and NCBI sequences of BC065744 and BC053632 are shown.

(F) A549 cells were infected with WSN at indicated mois for 12 hr or at an moi of 3 for indicated hours. RT-PCR was performed to determine the NRAV expression.

(G) The NRAV expression in indicated human cell lines infected with/without WSN (moi = 3) for 12 hr was examined by RT-PCR. The viral nucleoprotein (NP) was examined by western blotting.

(H and I) The NRAV expression was detected in cells infected with Sendai virus (SeV), Muscovy duck reovirus (MDRV), or herpes simplex virus (HSV) by RT-PCR (H) and qRT-PCR (I).

Shown are representative RT-PCR results from three independent experiments. Data are shown as means ± SEM (n = 3; *p < 0.05; **p < 0.01). See also Figure S1 and Table S1.

Expression of Human NRAV Significantly Increases IAV Virulence in Transgenic Mice

Although we did not succeed in detecting mouse lncRNA NRAV, mouse genome contains the *nrav* homolog sequence. To further define the role of NRAV in IAV infection, we wished to establish a more physiological model system. For this, transgenic (TG) mice expressing human NRAV were generated as previously described (Wei et al., 2014). The transgenic founders with high NRAV expression in lung were selected (Figure 3A). The TG mice and wild-type (WT) litter-

altered expression of NRAV, and therefore NRAV functions unlikely through a *cis*-effect on DYNLL1 (Figures S2F and S2G). These data suggest that lncRNA NRAV is involved in regulating IAV replication, and downregulation of NRAV in infected cells might be a host self-protection response to the virus infection, which may be critical to viral clearance.

mates were intranasally inoculated with WSN virus, and the influence of NRAV on the virulence and infection kinetics was analyzed. As expected, the IAV showed a considerably higher virulence in TG mice than that in WT mice. Under our experimental condition, body weight loss of infected TG mice was observed on day 4 postinfection (dpi) (Figure 3B). By 5–9 dpi,
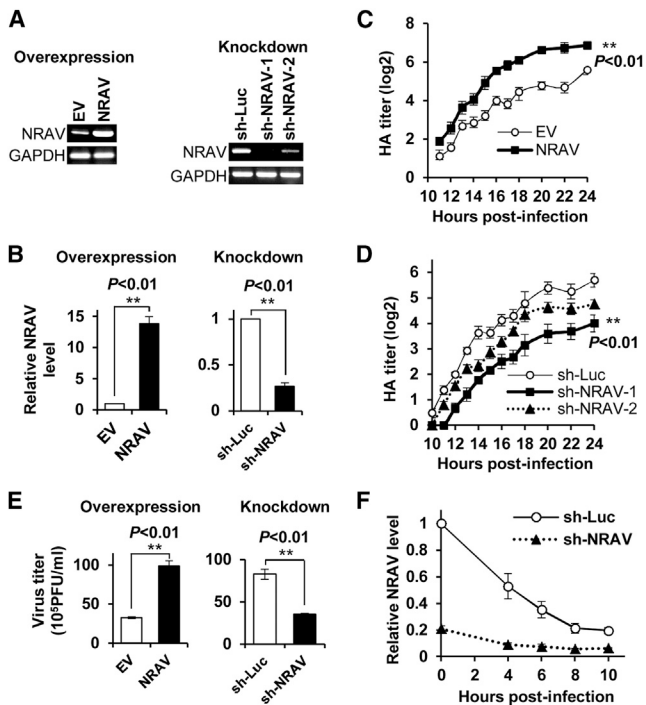
Figure 2. Altering NRAV Expression Has Profound Effects on IAV Replication in Human Cells

(A and B) The efficiency of NRAV overexpression and shRNA-based knockdown was determined by RT-PCR (A) in uninfected A549 cells or by qRT-PCR (B) in WSN infected A549 cells.

(C and D) IAV replication kinetics of NRAV-overexpressing (C) and NRAV knockdown (D) A549 cells were examined by hemagglutinin (HA) assay (moi = 0.3). The virus titers in supernatants were measured at indicated time points.

(E) IAV replication was examined by plaque assay. Virus titers in supernatants were measured at 16 hpi. Shown are representative results from infected overexpression cells (moi = 0.3) and knockdown cells (moi = 1).

(F) The expression of NRAV in infected NRAV knockdown cells was analyzed at indicated time (moi = 1) by qRT-PCR.

Cells expressing empty vector (EV) or luciferase shRNA (sh-Luc) were used as controls. n = 3; means ± SEM. See also Figure S2.

infected TG mice exhibited a consistent decrease in body weight, and with an average loss of approximately 25% on 8 dpi. All infected TG mice died within 9 dpi (Figure 3C). Under the same conditions, however, inoculated WT littermates started body weight loss on 5 dpi, with an average loss of approximately 8% on 8 dpi, and only approximately 40% of infected WT mice succumbed within 9 dpi (Figure 3C). Approximately 60% infected WT mice gained body weight gradually after 8 dpi and finally survived.

To further evaluate the in vivo effect of NRAV on IAV pathogenesis, we compared the viral loads and pathologies of the infected TG mice with WT littermates. Strikingly, the lung viral titer in TG mice was significantly higher than that in WT mice (Figure 3D), indicating more active replication of IAV in TG mice expressing NRAV. Remarkably, pathologic examination by hematoxylin and eosin (H&E) staining displayed more severe inflammation in the lungs of infected TG mice than those of the WT controls (Figure 3E). Together, these observations reveal that expression of lncRNA NRAV renders TG mice more susceptible to IAV infection.

NRAV Negatively Regulates the Expression of Several Critical ISGs

In an attempt to define the mechanism of NRAV affecting IAV replication, we performed a cDNA microarray to profile the cellular transcriptional response to NRAV overexpression in A549 cells infected with WSN for 16 hr. The microarray data displayed 882 genes upregulated and 1,538 genes downregulated (over 2-fold change, p < 0.05) in NRAV-overexpressing cells as compared with the controls (Figure 4A, left). Many of the differentially expressed genes were found to be associated with pathogen infection and viral reproduction through pathway analysis and Gene Ontology (GO) analysis (Figures S3A and S3B). Surprisingly, we identified 107 ISGs from differentially expressed genes in NRAV-overexpressing cells, and strikingly, the enrichment score of these ISGs was significantly high (21.3) using the analysis with interferome (Rusinova et al., 2013) (Table S2). Since ISGs are important antiviral effectors, we focused specifically on the ISG genes for further studies. Importantly, mRNA levels of some critical ISGs were significantly reduced in NRAV-overexpressing cells, including IFIT2, IFIT3, IFITM3, OASL, and MxA (Figure 4A, right). This finding was further confirmed by qRT-PCR (Figure 4B). In contrast, the mRNA levels of these ISGs were upregulated in NRAV knockdown cells (Figure 4C). Furthermore, the expression of ISGs regulated by NRAV was examined in IAV-infected NRAV TG mice and WT littermates. Consistently, we found that the levels of these ISGs in TG mice were significantly reduced as compared with those in WT controls after infection with IAV (Figures 4D and 4E). These results reveal that NRAV functions as a negative regulator of some ISGs during the IAV infection in vitro and in vivo.

Based on these data, we hypothesized that NRAV might impair host antiviral response through downregulation of some key ISGs, and if so, forced expression of these ISGs could reverse the effects of NRAV overexpression on IAV pathogenesis. To this end, exogenous IFIT2, IFIT3, IFITM3, or MxA was transiently expressed in the cell lines overexpressing NRAV or empty vector (EV) (Figure S3C). Indeed, forced expression of IFIT2, IFIT3, IFITM3, or MxA reversed the effect of NRAV on the IAV replication despite existence of excessive NRAV, whereas expression of control DDX3X, a component of TBK1-dependent innate immune response, had no such a function (Figures S3D and S3E). Because previous studies have shown that MxA interacts with IAV protein NP to inhibit the viral transcription (Mänz et al., 2013), we tested whether NRAV knockdown had any effects on IAV cRNA levels. Indeed, we found that the cRNA levels were clearly low in NRAV-depleted cells compared to the control at 8 hpi (Figure S3F), suggesting that the increased MxA caused by NRAV downregulation may block IAV transcription. However, altering NRAV expression has no significant effect on viral entry at early stage of viral infection (4 hr) (Figure S3G). These results suggest that lncRNA NRAV is critically involved in regulation of innate immune response via controlling the levels of several critical ISGs during the viral infection.

NRAV Suppresses MxA Expression Induced by Different Virus Infection and IFN Stimulation

Results presented above revealed that MxA levels were the most significantly affected by altering NRAV expression. To confirm
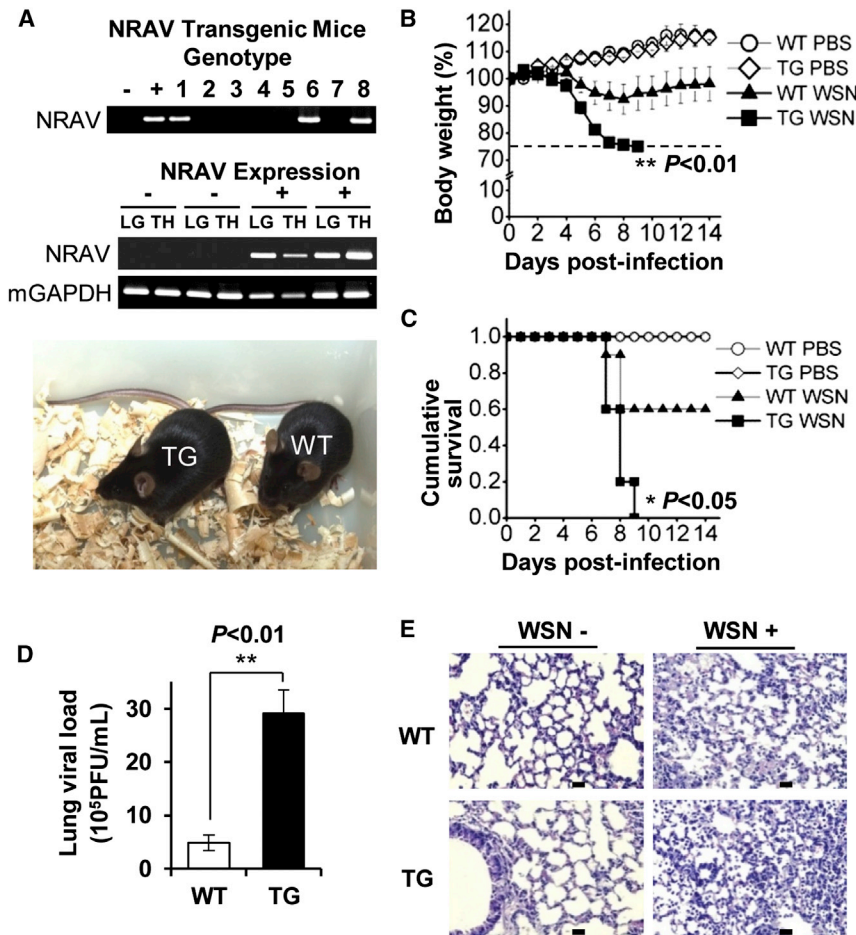
Figure 3. Expression of Human NRAV Significantly Increases IAV Virulence in Transgenic Mice

(A) The genotype (upper) and NRAV expression (middle) of C57BL/6J TG mice were determined by PCR of mouse tail DNA and RT-PCR of tissue RNA. −, WT littermates; +, TG mice; LG, lung; TH, thymus. Photo of TG and WT mice is shown (lower).

(B and C) The influence of NRAV on the WSN virulence and infection kinetics in mice were determined by body weight loss (B) and cumulative survival curve (C). Five- to six-week-old TG and WT mice were intranasally inoculated with 10^3 PFU of WSN (8–10 mice/group) or PBS (5 mice/group). The dashed line in (B) indicates the endpoint of 25% weight loss. Statistical significance in (C) was determined by log rank test.

(D) The lung viral loads in infected TG and WT mice as described in (B) were measured by plaque forming assay on day 6 (13 mice/group).

(E) Representative light photomicrographs of the mouse lung stained with HE on 6 dpi. The leukocyte infiltration was more pronounced in the infected TG mice in comparison with infected WT mice. Scale bars, 20 μm.

Data were shown as means ± SEM. *$p < 0.05$, **$p < 0.01$.

this finding, western blotting was performed to examine MxA protein. Similarly, we observed that MxA protein levels were markedly affected by altered NRAV expression (Figure S4A). Thus, MxA was selected for further studies. To further define the functional involvement of NRAV in regulating MxA expression, we investigated the effect of NRAV on MxA expression induced by different virus infections or stimulations. Interestingly, overexpression of NRAV resulted in a significant decrease in MxA expression in all cells infected with SeV for 12 hr or MDRV or HSV for 24 hr (Figures 5A–5C and S4B–S4D). In addition, when the cells were stimulated with bacterial lipopolysaccharides (LPSs) for 3 hr, the MxA level in NRAV-overexpressing cells was also significantly reduced as compared with the control cells (Figures S4E and S4F).

Because virus-induced MxA expression is regulated by cytokine-activated JAK/STAT1 signaling, we determined whether NRAV had any effects on the activation of this signaling. To test this possibility, phosphorylation of STAT1 was examined by western blotting. Surprisingly, no significant difference in the levels of p-STAT1 was observed between the infected NRAV-overexpressing cells and the control cells (Figure 5D). Our previous and current studies showed that A549 cells ectopically expressing with or without NRAV are capable of producing IFNs (Wei et al., 2014) (Figure S4G). Thus, we tested whether NRAV had effects on total cytokine levels secreted by infected

cells. Consistently, no significant difference in MxA levels was detected in the fresh A549 cells stimulated with supernatants derived from either IAV-infected NRAV-overexpressing cells or infected control cells (Figures S4H and S4I, left). A similar result was obtained from the NRAV-depleted cells and the control cells (Figure S4I, right). Additionally, we found that the expression of MxA induced by IFN-β or IL29 was significantly reduced in the NRAV-overexpressing cells compared with the control (Figures 5E, 5F, S4J, and S4K). Together, these results reveal that NRAV negatively regulates MxA expression in response to broad stimulations without significantly altering total cytokine production and JAK/STAT1 signaling.

NRAV Inhibits the Initial Transcription of MxA and IFITM3, Likely through Regulating Histone Modifications of the ISG Genes

Next, we investigated how NRAV might regulate the ISG expression. To this end, we determined the cellular localization of NRAV and found that although NRAV was localized both in the cytoplasm and nucleus, more NRAV was distributed in the nucleus of A549 cell (Figures 6A and S5A). Thus, we presumed that NRAV might be involved in transcriptional control of these ISGs. The pre-mRNA level can represent the initial transcription rate. Therefore, the primers to examine the pre-mRNA levels of MxA (preMxA) and IFITM3 (preIFITM3) were designed as previously described (Zeisel et al., 2011) (Figure 6B). We observed that the preMxA and preIFITM3 levels in infected NRAV-overexpressing cells were lower than those in control ($p < 0.05$), while no bands were observed in no reverse transcriptase control
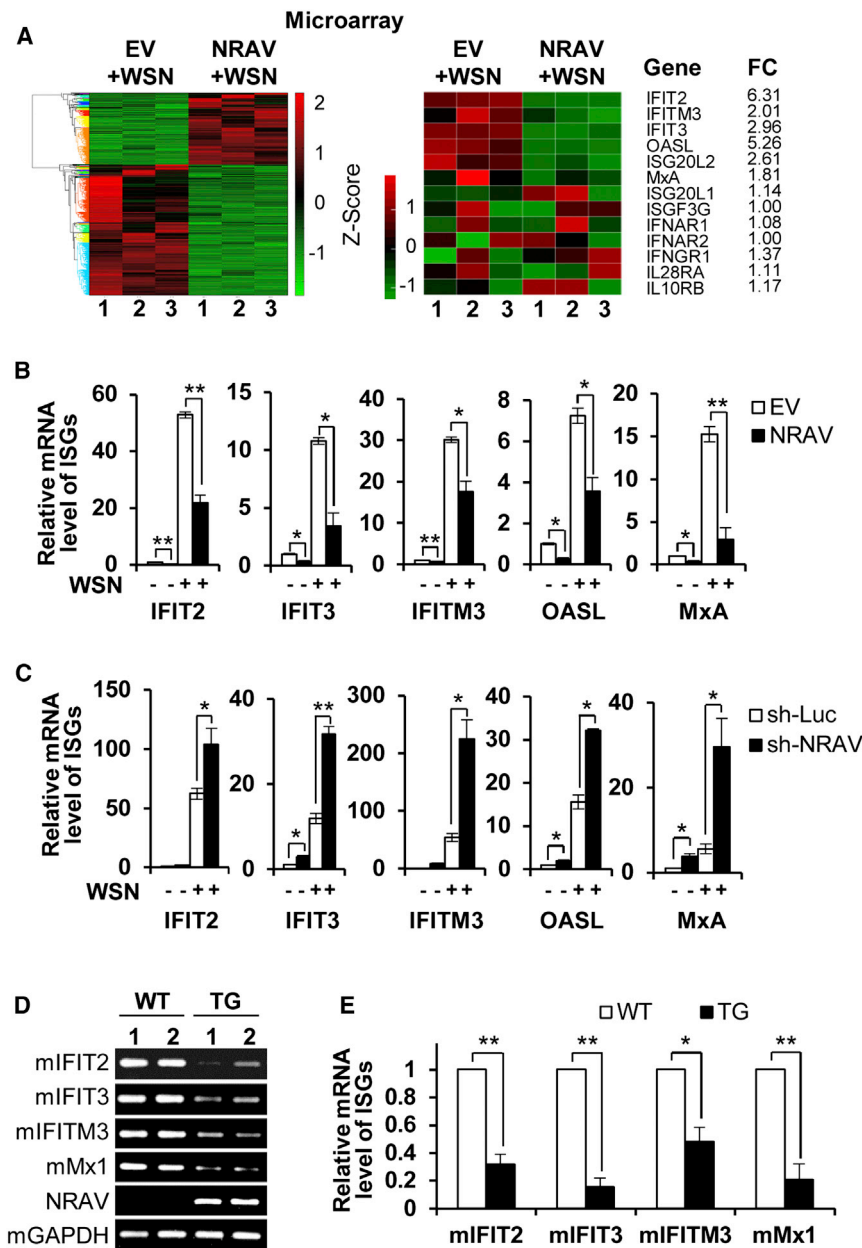
Figure 4. NRAV Negatively Regulates the Expression of Several Critical ISGs

(A) cDNA microarray analysis displayed hundreds of genes differentially expressed (n = 3, fold change > 2.0, p < 0.05) in WSN infected NRAV-overexpressing cells compared with control (moi = 3; 16 hpi) (left). Significantly changed ISGs and unchanged ISGs and IFN receptors are shown (right). The RNA quantitation data are shown as centered and scaled log2 data in heatmaps.

(B and C) The mRNA levels of ISGs in NRAV-expressing and EV control cells (B) or NRAV knockdown and sh-Luc control cells (C) infected with or without WSN were determined by qRT-PCR (n = 3).

(D and E) The mRNA levels of mIFIT2, mIFIT3, mIFITM3, and mMx1 in infected TG or WT mouse lungs were determined by RT-PCR (D) or by qRT-PCR (E). In (D), 1 and 2 indicate two individuals. Data are shown as means ± SEM. *p < 0.05, **p < 0.01. See also Figure S3 and Table S2.

expression of MxA was still inhibited in the presence of NRAV. In addition, we examined the mRNA decay rate of MxA in the infected cells treated with actinomycin D (ActD), since lncRNAs can activate mRNA decay through recruiting STAU1 to mRNAs (Kretz et al., 2013). No significant difference in the mRNA degradation rates was detected between NRAV-overexpressing cells and control cells (Figures S5F and S5G). These data indicate that NRAV may be not associated with MxA DNA methylation and post-transcriptional regulation of MxA.

Histone modification at transcription start sites is a crucial step for the regulation of gene transcription, and previous studies have proposed that lncRNAs are involved in these processes (Wang and Chang, 2011). Next, we investigated the histone 3 lysine 4 trimethylation (H3K4me3) as an active mark and histone 3 lysine 27 trimethylation (H3K27me3) as a repression signal by performing chromatin immunoprecipitation (ChIP). We found that the H3K4me3 enrichments at the *mxA* and *ifitm3* transcription start sites in NRAV-overexpressing cells were obviously impaired as compared with those in control cells following IAV infection (Figures 6F and S5H). In contrast, the H3K27me3 enrichment at *mxA* gene locus in infected NRAV-overexpressing cells exhibited remarkably higher than that in control cells, although the H3K27me3 enrichment at *ifitm3* remained unchanged (Figures 6G and S5I). Consistently, NRAV knockdown resulted in a significant increase in H3K4me3 enrichments and a significant decrease in H3K27me3 enrichments at *mxA* and *ifitm3* transcription start sites (Figures S5J and S5K). These data reveal that NRAV may function to inhibit the ISG transcription by affecting the histone modifications of these genes.

(Figures 6C–6E), indicating that NRAV may regulate the initial transcription of MxA and IFITM3. Furthermore, we observed that the promoter activity of both MxA and IFITM3 was significantly reduced in NRAV-overexpressing cells compared with control cells using a luciferase reporter assay (Figures S5B–S5D). These observations suggest that NRAV may be involved in negative regulation of promoter function of these ISGs.

Because lncRNAs were shown to silence gene transcription through maintenance of DNA methylation (Mohammad et al., 2012) and *mxA* contains a low CpG promoter (Ramirez-Carrozzi et al., 2009), we determined whether NRAV affected the DNA methylation of *mxA* gene. As shown in Figure S5E, treatment of A549 cells with DNA methyltransferase inhibitor decitabine (DAC) resulted in an increase of MxA mRNA level. However,
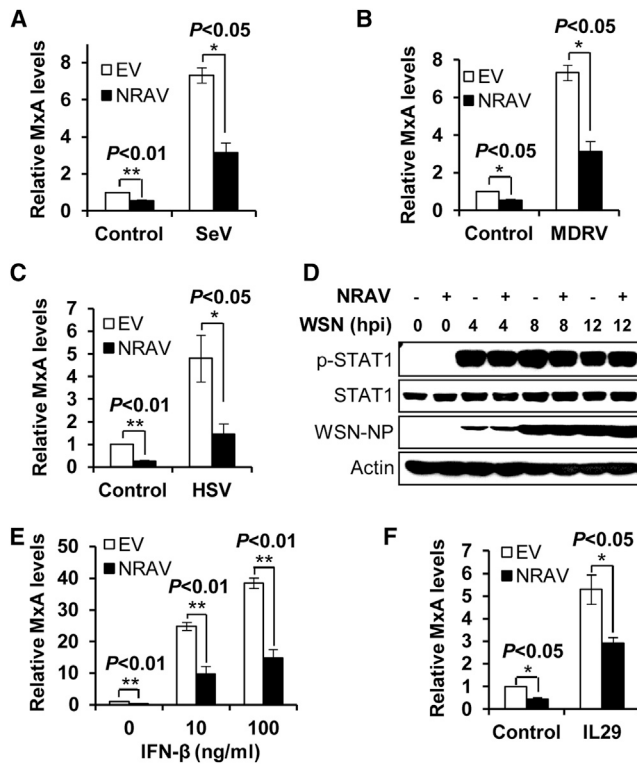
Figure 5. NRAV Suppresses MxA Expression Induced by Different Virus Infection and IFN Stimulation

(A–C) The MxA mRNA levels in following NRAV cells and EV cells were determined by qRT-PCR: SeV infected A549 cells (A), MDRV infected 293T cells (B), and HSV infected A549 cells (C) (means ± SEM; n = 3).

(D) A549 cells overexpressing NRAV or control were infected with WSN for indicated time. STAT1 and its Tyr701-phosphorylation were determined by western blotting.

(E and F) The MxA mRNA levels in NRAV overexpressing cells and control A549 cells stimulated by IFN-β (E) or IL29 (F) (50 ng/ml) for 3 hr were detected by qRT-PCR (means ± SEM; n = 3). *p < 0.05, **p < 0.01. See also Figure S4.

To further identify the functional protein partners of NRAV, we performed RNA pull-down by using biotinylated NRAV antisense probes or scramble control probes. Interestingly, a specific NRAV-bound protein in resting A549 cells was pulled down and identified to be ZO-1-associated nucleic acid binding protein (ZONAB) by mass spectrometry (Figures 6H and S6A; Table S3). This finding was further confirmed by RNA immunoprecipitation (RIP) showing that the amount of NRAV precipitated with anti-ZONAB Ab was dramatically higher than that of GAPDH control (Figure S6B). We next determined the role of ZONAB in MxA expression. The shRNA-based ZONAB knockdown was performed and verified by qRT-PCR (Figure S6C). Interestingly, the levels of MxA mRNA were significantly decreased after silencing ZONAB in both infected and uninfected cells (Figure 6I). When ZONAB was depleted in NRAV-overexpressing cells, the MxA mRNA was decreased to a lower level (Figure 6J), while NRAV was not affected by altered ZONAB expression (Figure S6D, left). Consistently, the exogenous expression of ZONAB in NRAV-overexpressing cells partially reversed the NRAV-mediated suppression of MxA expression (Figures

S6D–S6F). These results indicate that ZONAB is involved in MxA transcription as a positive regulator.

The Spatial Structure of Functional Moieties Was Essential for lncRNA NRAV Function

The diverse functions of lncRNAs are based on their propensity to fold into thermodynamically stable secondary and higher-order structures (Mercer and Mattick, 2013). To determine the functional structures of lncRNA NRAV, we designed and constructed eight truncation and deletion mutants based on the predicted secondary structure of NRAV through three softwares, RNAfold (Gruber et al., 2008), Centroidfold, and Genebee (Figures 7A and 7B). As displayed, mutant A (mutA) lacks the stem-loop arm A, while contains other stem-loop structures or elements (arms C, D, and E) as compared with the intact NRAV (Figure 7A). Ectopic expression of these mutants was determined by RT-PCR (Figure 7B, right). Interestingly, experiments testing the effects of these mutants on virus replication demonstrated that all examined structure moieties of NRAV except arm D, which was a small arm of NRAV (nt 618–872), were required for its role in controlling IAV replication (Figure 7C). Consistently, the reduction of MxA mRNA level was detected only in cells ectopically expressing WT NRAV or its mutD (Figure 7D). These experiments demonstrate that RNA sequences of stem loops in NRAV except nt 618–872 may form a spatial structure that is essential for its function.

DISCUSSION

Although much emphasis has been placed on investigating host protein factors in the activation of innate immune responses to IAV infection, little is known about the role of lncRNAs in these processes. lncRNA THRIL, NeST, NEAT, and lincRNA-Cox2 have been reported to regulate the expression of TNF-α, IFN-γ, IL8, and inflammatory response, respectively (Carpenter et al., 2013; Gomez et al., 2013; Imamura et al., 2014; Li et al., 2014). Here we report a human lncRNA named as NRAV, which is expressed in various human cells, but significantly downregulated during the IAV infection and infections with ssRNA virus (SeV), dsRNA virus (MDRV), and DNA virus (HSV). Importantly, we have revealed that overexpression of NRAV promotes the IAV replication in vitro and in vivo by suppressing the expression of several key ISGs, such as IFIT2, IFIT3, IFITM3, and MxA, very likely through affecting the histone modifications of these ISG genes. These findings establish that NRAV functions as an important regulatory molecule via negatively regulating the expression of some crucial antiviral proteins, which modulates the host innate immune response against IAV infection and maybe more broadly involved in other viral infections.

In uninfected cells, NRAV likely contributes to precise control of the expression of these critical ISGs. When virus infection is sensed, the reduction of NRAV would benefit the rapid accumulation of the antiviral proteins to facilitate the clearance of virus. Therefore, downregulation of NRAV may be initiated by host as a self-protection response. This is coherent with the tight and exquisite control of antiviral response that ensures rapid defense against pathogens with minimal inflammatory damage. A number of negative regulators of innate immunity have been found, such as SOCS1 and SOCS3, which negatively regulate
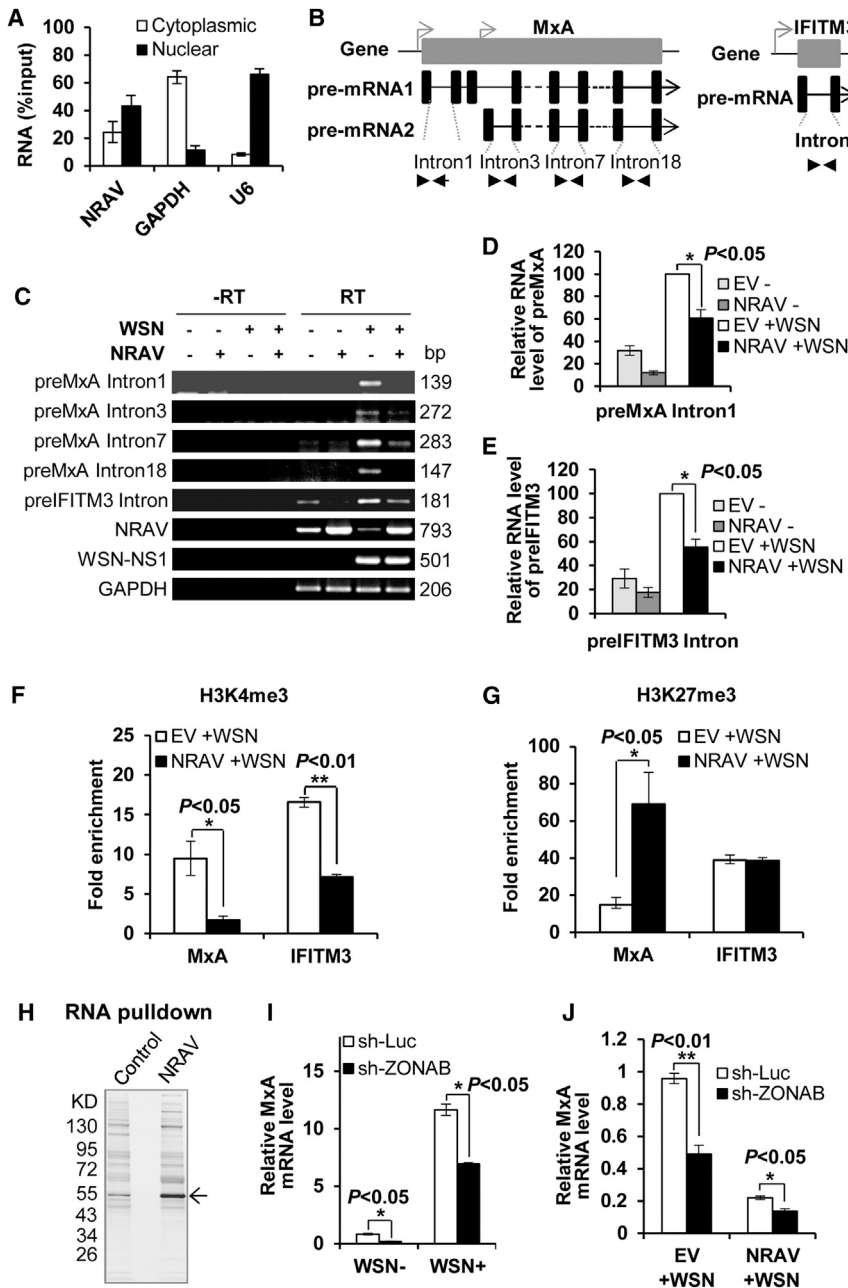
Figure 6. NRAV Inhibits the Initial Transcription of MxA and IFITM3 through Regulating Histone Modifications of the ISG Genes

(A) The RNA levels of NRAV, cytoplasmic control (GAPDH mRNA), and nuclear control (U6 RNA) were assessed by qRT-PCR in cytoplasmic and nuclear fractions from A549. The total RNA was used as input control. Data are shown as % input (means ± SEM; n = 3.)

(B) Paradigms of the pre-mRNA stuctures of MxA (left) and IFITM3 (right) (not scaled). Introns (black line) between two exons (black block) used for pre-mRNA detection are indicated. Several pairs of primers were used to detect two isoforms of pre-MxA. Corresponding primers are shown as a pair of arrows. Promoters are shown as bended arrows.

(C–E) The pre-mRNA levels of MxA (preMxA) and IFITM3 (preIFITM3) in IAV infected NRAV-overexpressing cells or EV control cells were determined by RT-PCR (C) and qRT-PCR (preMxA [D], preIFITM3 [E]). Shown are representative data of three independent experiments. Means ± SEM; n = 3. *p < 0.05. −RT, no reverse transcriptase in reverse transcription (RT). RT, normal reaction. The length of RT-PCR product is shown.

(F and G) ChIP analysis of H3K4me3 (F) and H3K27me3 (G) levels at the *mxA* and *ifitm3* locus in IAV-infected NRAV-overexpressing or control cells. The relative amounts of *mxA* and *ifitm3* DNA immunoprecipitated by the anti-H3K4me3 or anti-H3K27me3 antibody were normalized to that isolated by the control IgG. The fold enrichment was calculated as $2^{-\Delta\Delta Ct}$ (mean ± SEM; n = 3).

(H) Silver staining of proteins pulled down by NRAV antisense probes or scramble control probes from A549 cell lysate. The specific NRAV-associated band (arrow) was excised for mass spectrometry. Shown are representative data from three independent experiments.

(I) MxA mRNA levels in ZONAB-depleted A549 cells infected with or without WSN (moi = 1, 12 hpi) were measured by qRT-PCR and normalized to that of uninfected control cells transfected with vector sh-Luc.

(J) Experiments were performed as described in (I). MxA mRNA levels in ZONAB-depleted NRAV-overexpressing A549 cells were measured by qRT-PCR.

Data are shown as means ± SEM; n = 3. *p < 0.05, **p < 0.01. See also Figures S5–S7 and Table S3.

IFN-activated JAK-STAT signaling to control the ISG transcriptional response to IFN stimulation (Akhtar and Benveniste, 2011). LincRNA-Cox2 also mediates the repression of some immune genes (Carpenter et al., 2013). Although the mechanism underlying downregulation of NRAV by viral infection remains elusive, the expression of NRAV is likely controlled by particular pathways activated upon sensing the viral infection. Indeed, we found that the NRAV downregulation was induced only by viral RNA which is produced during virus replication (Figures S7A–S7E) and newly synthesized protein(s) (Figure S7F). However, these proteins might include neither virus-induced cytokines nor IFNAR1 (Figures S7G–S7J). We observed that reduction of NRAV was not caused by increase in RNA decay (Figure S7K),

indicating that this protein(s) might be relevent with the transcriptional regulation of NRAV. CpG islands and some transcription factor binding sites on the upstream of *nrav* were predicted (Figure S7L). Interestingly, DNA methyltransferase might participate in the regulation of NRAV (Figures S7M–S7P). These findings suggest that virus infection might induce the transcription inhibition of *nrav* through epigenetic modification.

We identified that NRAV critically regulated several key antiviral effectors in innate immunity. Strikingly, the transcriptional regulations of these genes are distinct, and multiple mechanisms are involved. For example, MxA/Mx1 is regulated through strictly IFN-dependent pathway, while IFIT2 and IFIT3 are through both IFN-dependent and IFN-independent pathways
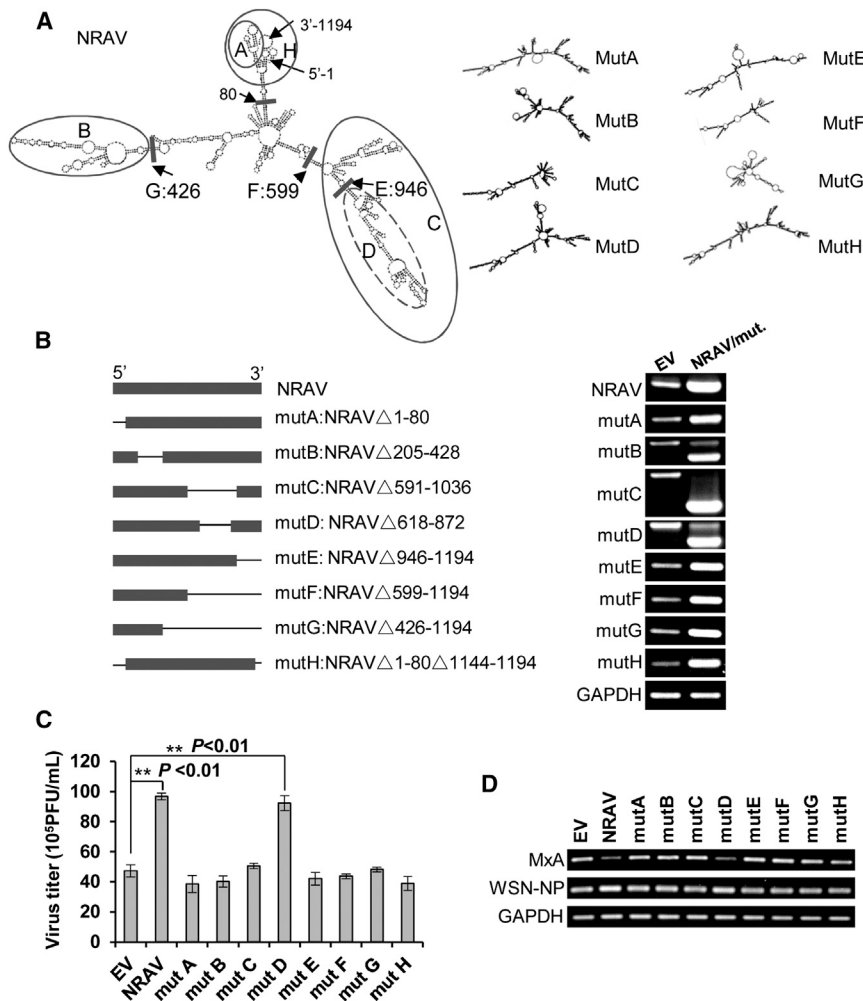
Figure 7. The Spatial Structure of Functional Moieties Was Essential for lncRNA NRAV Activity

(A) Secondary structure predictions of NRAV and mutations were performed through three softwares (RNAfold, Certroidfold, and Genebee). The mutation locations were labeled by circle or short bar.

(B) Schematic diagram of truncation and deletion mutations of NRAV is shown (left). The stable exogenous expression of NRAV or its mutants in A549 cells was determined by RT-PCR (right).

(C) A549 cells expressing NRAV or its mutants were infected with IAV, and the virus titers in culture supernatants were determined through plaque-forming assay (n = 3; means ± SEM; **p < 0.01).

(D) The MxA mRNA levels in A549 cells in (C) were detected by RT-PCR. Shown are representative results from three independent experiments.

that regulates transcription of cyclin D1 and PCNA as an important transcription factor and posttranscriptionally regulates other protein and mRNA levels in cytoplasm (Lima et al., 2010; Nie et al., 2012). Although it is unclear whether ZONAB functions as a transcription factor of ISG expression, we found a ZONAB binding sequence (invert CCAAT) at −219 to −215 of MxA transcription start region (Dolfini and Mantovani, 2013), suggesting the potential involvement of ZONAB in initial transcription of MxA. Additionally, as a transcription factor ZONAB might also be involved in histone modifications and nucleosome packing

(Lazear et al., 2013). Interestingly, these NRAV-modulated ISGs have recently been reported belonging to a subset of ISGs which are regulated by an IKKi-associated specific signal pathway (Ng et al., 2011; Tenoever et al., 2007). In this study, we found that the initial transcription rates of MxA and IFITM3 were reduced and the histone modifications (active mark H3K4me3 and repressive mark H3K27me3) were altered by NRAV. Several lncRNAs have been reported to regulate chromatin remodeling on specific gene location through directly binding with hnRNPs (Carpenter et al., 2013; Li et al., 2014). Although we have excluded the possibility that NRAV functions through regulating IFN-JAK/STAT1 pathway, the molecular mechanism by which NRAV regulates the initial transcription and histone modifications remains unknown. On the other hand, NRAV was shown to interfere with the MxA and IFITM3 promoter activity in a luciferase reporter system. These data suggest that there might exist multiple mechanisms underlying NRAV-mediated regulation of ISG transcription.

It has been thought that lncRNAs usually interact with other molecules to exert regulatory activities. In this study, ZONAB was identified as a NRAV-associated protein involved in MxA transcription regulation. ZONAB is a multifunctional protein

(Rothenberg, 2014). It has been thought that ZONAB can upregulate several chromatin remodeling components (histone H4 and HMG-I) and MYC that recruits core histone-modifying enzymes to DNA (Sourisseau et al., 2006). Further experiments are needed in the future to address how ZONAB interacts with NRAV to regulate ISG expression.

Human NRAV is an intronic antisense lncRNA of dynein light-chain gene *dynll1*. Although Dynein is shown to be recruited by many viruses to facilitate their replication and enhance their spread, and direct interaction of Dynll with virions is identified (Merino-Gracia et al., 2011), we did not observe significant change in the Dynll1 levels after altering the NRAV expression (GEO accession number GSE48874; Figures S2F and S2G). Of interest is that hundreds of genes differentially expressed in NRAV-overexpressing cells and the pathway and GO analysis indicated that many are associated with pathogen infection and viral reproduction. In addition, the expression of NRAV in different types of human cells also indicates its broad functions. The expression of human NRAV in multiple tissues of TG mice including lung, thymus, and bone marrow might be important for the IAV pathogenesis. Therefore, the role of NRAV may be not limited to the modulation of ISGs. Moreover, the decline of

NRAV level can also be induced by other RNA/DNA virus infections. Hence, we surmise that NRAV-related cellular response may be a universal defense against virus infection. The exact relationship between NRAV distribution in different tissues and its antiviral activities needs to be determined.

EXPERIMENTAL PROCEDURES

Microarray and Data Analysis

The lncRNA cDNA microarray was from Arraystar (Arraystar, Rockville, MD). The cDNA microarray was performed using Human 12x135K gene expression microarray (Roche NimbleGen, Madison, WI). Total RNAs from three independent groups of WSN-infected A549 cells or control cells were prepared using Trizol reagent (Invitrogen, Carlsbad, CA). cDNA synthesis, labeling, hybridization, and data analysis were carried out as previously described (Guo et al., 2014) (see Supplemental Information).

Cells, Viruses, Antibodies, and Plasmids

Cells, viruses, and antibodies were described in the Supplemental Information. For plasmid construction, human IFIT2, IFIT3, IFITM3, MxA, and DDX3X were subcloned into the pcDNA3.1 and pCMV5a vectors. shRNA-based knockdown plasmids were generated with a pSIH-H1-GFP lentiviral vector expressing shRNA.

Viral Infection and Virus Titers Assay

A549 cells were infected with IAV WSN, Sendai virus (SeV), or herpes simplex virus (HSV), and 293T cells were infected with Muscovy duck reovirus (MDRV). Virus titers in supernatants were determined (see Supplemental Information).

5′ and 3′ RACE

The 5′ and 3′ RACE analyses were performed using the SMARTer RACE cDNA amplification Kit (Clontech) as per the manufacturer's instructions. RACE PCR products were cloned into pZeroBack (Tiangen, Beijing, China) and sequenced.

Transgenic Mice and Virus Challenge

The mouse experimental design and protocols used in this study were approved by the Research Ethics Committee of Institute of Microbiology, Chinese Academy of Sciences (permit number PZIMCAS2012001). The studies of mice were performed in strict accordance with the Regulation of Institutional Research Ethics Committee of Institute of Microbiology. The NRAV transgenic C57BL/6 mice were created as previously described (Wang et al., 2014; Wei et al., 2014). Mice were inoculated intranasally with WSN. Mouse lungs were collected for lung viral loads assay and H&E staining (see Supplemental Information).

RNA Pull-Down Assay, RNA Immunoprecipitation, and Chromatin Immunoprecipitation

Uninfected A549 cell lysates were used for RNA pull-down assay and RIP, and IAV-infected A549 cells were subjected to ChIP assays using the Magna ChIP A/G chromatin immunoprecipitation kit (Millipore) following the manufacturer's instruction as described in Supplemental Information.

Generation of Stable Cell Lines and Cell Stimulation

The stable NRAV-overexpressing cells and A549 cell lines stably expressing specific ISGs were generated with a retroviral expression system by infecting the cells with retroviruses encoding these genes. Recombinant human IFN-β and IL29 were purchased from PeproTech (Rocky Hill, NJ). For stimulation, unless indicated, cells were incubated for 2–3 hr with the recombinant cytokines or peptides (see Supplemental Information).

Western Blotting and Northern Blotting

For western blotting, cell lysates were separated by SDS-polyacrylamide gel electrophoresis, transferred onto a nitrocellulose membrane, and probed with indicated antibodies as described previously (Wei et al., 2014). For northern blotting, total RNA of A549 cell was isolated using Trizol reagent. Probe is a DNA fragment of NRAV (793 bp, 358–1,150), which was radiolabeled by using Prime-a-Gene Labeling System (Promega). The assay was performed by using Northernmax-gly kit (Invitrogen) and autoradiography.

Statistical Analysis

Comparison between groups was made using Student's t test. Data represent the mean ± SEM. Differences were considered statistically significant with $p < 0.05$.

ACCESSION NUMBERS

The GenBank accession number for the *nrav* gene sequence reported in this paper is KF311770. The Gene Expression Omnibus accession numbers for the microarray data reported in this paper are GSE32878 and GSE48874.

SUPPLEMENTAL INFORMATION

Supplemental Information includes seven figures, three tables, and Supplemental Experimental Procedures and can be found with this article at http://dx.doi.org/10.1016/j.chom.2014.10.001.

REFERENCES

Akhtar, L.N., and Benveniste, E.N. (2011). Viral exploitation of host SOCS protein functions. J. Virol. *85*, 1912–1921.

Carpenter, S., Aiello, D., Atianand, M.K., Ricci, E.P., Gandhi, P., Hall, L.L., Byron, M., Monks, B., Henry-Bezy, M., Lawrence, J.B., et al. (2013). A long noncoding RNA mediates both activation and repression of immune response genes. Science *341*, 789–792.

Cullen, B.R. (2013). Making a NeST for a persistent virus. Cell Host Microbe *13*, 241–242.

Dolfini, D., and Mantovani, R. (2013). Targeting the Y/CCAAT box in cancer: YB-1 (YBX1) or NF-Y? Cell Death Differ. *20*, 676–685.

Everitt, A.R., Clare, S., Pertel, T., John, S.P., Wash, R.S., Smith, S.E., Chin, C.R., Feeley, E.M., Sims, J.S., Adams, D.J., et al.; GenISIS Investigators; MOSAIC Investigators (2012). IFITM3 restricts the morbidity and mortality associated with influenza. Nature *484*, 519–523.

Fensterl, V., Wetzel, J.L., Ramachandran, S., Ogino, T., Stohlman, S.A., Bergmann, C.C., Diamond, M.S., Virgin, H.W., and Sen, G.C. (2012). Interferon-induced Ifit2/ISG54 protects mice from lethal VSV neuropathogenesis. PLoS Pathog. *8*, e1002712.

Gomez, J.A., Wapinski, O.L., Yang, Y.W., Bureau, J.F., Gopinath, S., Monack, D.M., Chang, H.Y., Brahic, M., and Kirkegaard, K. (2013). The NeST long

ncRNA controls microbial susceptibility and epigenetic activation of the interferon-γ locus. Cell *152*, 743–754.

Gruber, A.R., Lorenz, R., Bernhart, S.H., Neuböck, R., and Hofacker, I.L. (2008). The Vienna RNA websuite. Nucleic Acids Res. *36* (Web Server issue), W70–W74.

Guo, G., Kang, Q., Zhu, X., Chen, Q., Wang, X., Chen, Y., Ouyang, J., Zhang, L., Tan, H., Chen, R., et al. (2014). A long noncoding RNA critically regulates Bcr-Abl-mediated cellular transformation by acting as a competitive endogenous RNA. Oncogene. http://dx.doi.org/10.1038/onc.2014.131.

Guttman, M., and Rinn, J.L. (2012). Modular regulatory principles of large noncoding RNAs. Nature *482*, 339–346.

Imamura, K., Imamachi, N., Akizuki, G., Kumakura, M., Kawaguchi, A., Nagata, K., Kato, A., Kawaguchi, Y., Sato, H., Yoneda, M., et al. (2014). Long noncoding RNA NEAT1-dependent SFPQ relocation from promoter region to paraspeckle mediates IL8 expression upon immune stimuli. Mol. Cell *53*, 393–406.

Kretz, M., Siprashvili, Z., Chu, C., Webster, D.E., Zehnder, A., Qu, K., Lee, C.S., Flockhart, R.J., Groff, A.F., Chow, J., et al. (2013). Control of somatic tissue differentiation by the long non-coding RNA TINCR. Nature *493*, 231–235.

Lazear, H.M., Lancaster, A., Wilkins, C., Suthar, M.S., Huang, A., Vick, S.C., Clepper, L., Thackray, L., Brassil, M.M., Virgin, H.W., et al. (2013). IRF-3, IRF-5, and IRF-7 coordinately regulate the type I IFN response in myeloid dendritic cells downstream of MAVS signaling. PLoS Pathog. *9*, e1003118.

Li, Z., Chao, T.C., Chang, K.Y., Lin, N., Patil, V.S., Shimizu, C., Head, S.R., Burns, J.C., and Rana, T.M. (2014). The long noncoding RNA THRIL regulates TNFα expression through its interaction with hnRNPL. Proc. Natl. Acad. Sci. USA *111*, 1002–1007.

Lima, W.R., Parreira, K.S., Devuyst, O., Caplanusi, A., N'kuli, F., Marien, B., Van Der Smissen, P., Alves, P.M., Verroust, P., Christensen, E.I., et al. (2010). ZONAB promotes proliferation and represses differentiation of proximal tubule epithelial cells. J. Am. Soc. Nephrol. *21*, 478–488.

Lin, M.F., Jungreis, I., and Kellis, M. (2011). PhyloCSF: a comparative genomics method to distinguish protein coding and non-coding regions. Bioinformatics *27*, i275–i282.

Liu, X.Y., Chen, W., Wei, B., Shan, Y.F., and Wang, C. (2011). IFN-induced TPR protein IFIT3 potentiates antiviral signaling by bridging MAVS and TBK1. J. Immunol. *187*, 2559–2568.

Mänz, B., Dornfeld, D., Götz, V., Zell, R., Zimmermann, P., Haller, O., Kochs, G., and Schwemmle, M. (2013). Pandemic influenza A viruses escape from restriction by human MxA through adaptive mutations in the nucleoprotein. PLoS Pathog. *9*, e1003279.

Mercer, T.R., and Mattick, J.S. (2013). Structure and function of long noncoding RNAs in epigenetic regulation. Nat. Struct. Mol. Biol. *20*, 300–307.

Mercer, T.R., Dinger, M.E., and Mattick, J.S. (2009). Long non-coding RNAs: insights into functions. Nat. Rev. Genet. *10*, 155–159.

Merino-Gracia, J., García-Mayoral, M.F., and Rodríguez-Crespo, I. (2011). The association of viral proteins with host cell dynein components during virus infection. FEBS J. *278*, 2997–3011.

Mohammad, F., Pandey, G.K., Mondal, T., Enroth, S., Redrup, L., Gyllensten, U., and Kanduri, C. (2012). Long noncoding RNA-mediated maintenance of DNA methylation and transcriptional gene silencing. Development *139*, 2792–2803.

Ng, S.L., Friedman, B.A., Schmid, S., Gertz, J., Myers, R.M., Tenoever, B.R., and Maniatis, T. (2011). IκB kinase epsilon (IKK(epsilon)) regulates the balance between type I and type II interferon responses. Proc. Natl. Acad. Sci. USA *108*, 21170–21175.

Nie, M., Balda, M.S., and Matter, K. (2012). Stress- and Rho-activated ZO-1-associated nucleic acid binding protein binding to p21 mRNA mediates stabilization, translation, and cell survival. Proc. Natl. Acad. Sci. USA *109*, 10897–10902.

Peng, X., Gralinski, L., Armour, C.D., Ferris, M.T., Thomas, M.J., Proll, S., Bradel-Tretheway, B.G., Korth, M.J., Castle, J.C., Biery, M.C., et al. (2010). Unique signatures of long noncoding RNA expression in response to virus infection and altered innate immune signaling. mBiol. *1*, e00206–e00210.

Ramirez-Carrozzi, V.R., Braas, D., Bhatt, D.M., Cheng, C.S., Hong, C., Doty, K.R., Black, J.C., Hoffmann, A., Carey, M., and Smale, S.T. (2009). A unifying model for the selective regulation of inducible transcription by CpG islands and nucleosome remodeling. Cell *138*, 114–128.

Rothenberg, E.V. (2014). The chromatin landscape and transcription factors in T cell programming. Trends Immunol. *35*, 195–204.

Rusinova, I., Forster, S., Yu, S., Kannan, A., Masse, M., Cumming, H., Chapman, R., and Hertzog, P.J. (2013). Interferome v2.0: an updated database of annotated interferon-regulated genes. Nucleic Acids Res. *41* (Database issue), D1040–D1046.

Smale, S.T. (2012). Transcriptional regulation in the innate immune system. Curr. Opin. Immunol. *24*, 51–57.

Sourisseau, T., Georgiadis, A., Tsapara, A., Ali, R.R., Pestell, R., Matter, K., and Balda, M.S. (2006). Regulation of PCNA and cyclin D1 expression and epithelial morphogenesis by the ZO-1-regulated transcription factor ZONAB/DbpA. Mol. Cell. Biol. *26*, 2387–2398.

Tenoever, B.R., Ng, S.L., Chua, M.A., McWhirter, S.M., García-Sastre, A., and Maniatis, T. (2007). Multiple functions of the IKK-related kinase IKKepsilon in interferon-mediated antiviral immunity. Science *315*, 1274–1278.

Wang, K.C., and Chang, H.Y. (2011). Molecular mechanisms of long noncoding RNAs. Mol. Cell *43*, 904–914.

Wang, T., Tian, C., Zhang, W., Luo, K., Sarkis, P.T., Yu, L., Liu, B., Yu, Y., and Yu, X.F. (2007). 7SL RNA mediates virion packaging of the antiviral cytidine deaminase APOBEC3G. J. Virol. *81*, 13112–13124.

Wang, S., Chi, X., Wei, H., Chen, Y., Chen, Z., Huang, S., and Chen, J.L. (2014). Influenza A virus-induced degradation of eukaryotic translation initiation factor 4B contributes to viral replication by suppressing IFITM3 protein expression. J. Virol. *88*, 8375–8385.

Wei, H., Wang, S., Chen, Q., Chen, Y., Chi, X., Zhang, L., Huang, S., Gao, G.F., and Chen, J.L. (2014). Suppression of interferon lambda signaling by SOCS-1 results in their excessive production during influenza virus infection. PLoS Pathog. *10*, e1003845.

Winterling, C., Koch, M., Koeppel, M., Garcia-Alcalde, F., Karlas, A., and Meyer, T.F. (2014). Evidence for a crucial role of a host non-coding RNA in influenza A virus replication. RNA Biol. *11*, 66–75.

Yin, Z., Guan, D., Fan, Q., Su, J., Zheng, W., Ma, W., and Ke, C. (2013). lncRNA expression signatures in response to enterovirus 71 infection. Biochem. Biophys. Res. Commun. *430*, 629–633.

Zeisel, A., Köstler, W.J., Molotski, N., Tsai, J.M., Krauthgamer, R., Jacob-Hirsch, J., Rechavi, G., Soen, Y., Jung, S., Yarden, Y., and Domany, E. (2011). Coupled pre-mRNA and mRNA dynamics unveil operational strategies underlying transcriptional responses to stimuli. Mol. Syst. Biol. *7*, 529.

Zhang, Q., Chen, C.Y., Yedavalli, V.S., and Jeang, K.T. (2013). NEAT1 long noncoding RNA and paraspeckle bodies modulate HIV-1 posttranscriptional expression. mBiol. *4*, e00596–e00512.